SNS Neutrino Flux Simulation: Technical Note v1.1

D. Rimal, M. McIntyre, and H. Ray[1]
[1] *University of Florida, Gainesville, 32611*
(Dated: February 12, 2015)

The Spallation Neutron Source (SNS) produces a large neutrino flux, with a well defined energy spectra, as a by-product of its regular operation. The neutrino flux with such well characterized energy spectra can provide highly desired sensitivity for neutrino oscillation and cross section experiments. A handful of such experiments plan to utilize these freely available neutrinos to investigate the neutrino cross section and search for sterile neutrinos. It is necessary to have a detailed understanding of the neutrino flux and the neutron background rates at several locations near the SNS target area. To serve for this purpose, a Monte Carlo simulation package based on GEANT4 framework, was developed by the neutrino physics group at University of Florida. We studied secondary charged meson and lepton production as well as their different decay modes. This document provides a general description of our simulation effort, and presents an estimate of the neutrino flux at different locations of interest near the SNS target.

I. INTRODUCTION

The Spallation Neutron Source (SNS) at ORNL provides pulsed neutron beams for neutron science research [1]. Energetic neutron beams are produced by bombarding a liquid mercury target with a 1.0 GeV proton beam. In addition to the spalled neutrons, the SNS also produces a large neutrino flux with a well characterized energy spectra. Most of these neutrinos are produced by the decay of pions/muons at rest within the Hg target, and hence have a well characterized energy spectra. Neutrino sources with such well defined flux can provide an environment for performing precision measurements of neutrino parameters. The uncertainty in the neutrino flux is one of the dominant contribution to the systematic errors in the neutrino experiments. The neutrinos at SNS are available for free since they are produced as a by-product during regular operation, and greatly reduce the construction cost required to build such neutrino sources. Hence, some experiments are being proposed to utilize these free neutrinos. One such experiment is the OscSNS experiment, which plans to probe $\bar{\nu_\mu} \to \bar{\nu_e}$ and $\nu_\mu \to \nu_e$ appearance along with ν_μ disappearance into sterile neutrinos. The OscSNS experiment also plans to make high precision measurement for $\nu_e C \to e^- N$ scattering and $\nu e^- \to \nu e^-$ elastic scattering cross section [2]. In addition, the COHERENT collaboration is planning on performing world's first measurements of low-energy coherent neutrino scattering [3]. A detailed understanding of the neutrino flux and the background is the most critical part of all proposed experiments. We developed a Monte Carlo simulation package based on GEANT4 [4] to investigate the neutrino flux and backgrounds at several locations of interest near the SNS target area. This note provides a detailed description of our ongoing simulation efforts.

II. OVERVIEW OF THE SIMULATION

The interaction of an energetic proton beam with a liquid Hg target produces charged mesons, predominantly pions. Because of the high stopping power of Hg, most of these pions, traversing through the target, come to rest within a few nano-seconds of their production. These stopped pions decay at rest (DAR) producing neutrinos in the following scheme:

$$\pi^+ \to \mu^+ + \nu_\mu \tag{1}$$
$$\pi^- \to \mu^- + \bar{\nu_\mu} \tag{2}$$

The muons decay as,

$$\mu^+ \to e^+ + \bar{\nu_\mu} + \nu_e \tag{3}$$
$$\mu^- \to e^- + \nu_\mu + \bar{\nu_e} \tag{4}$$

Although the dominant source of neutrinos at SNS is the DAR of the stopped pions/muons, a small fraction ($< 1\%$) of the charged pions/muons also decay in flight (DIF). Most of the negatively charged pions (π^-) are captured in the Hg target largely suppressing neutrino species from the π^- decay chains. We simulated charged meson production from the proton-Hg interaction, their successive decay to produce different flavor of neutrinos, and the transportation of these particles through target and SNS geometry. The physics interactions are modeled in pre-packaged GEANT4 physics lists, which are discussed later.

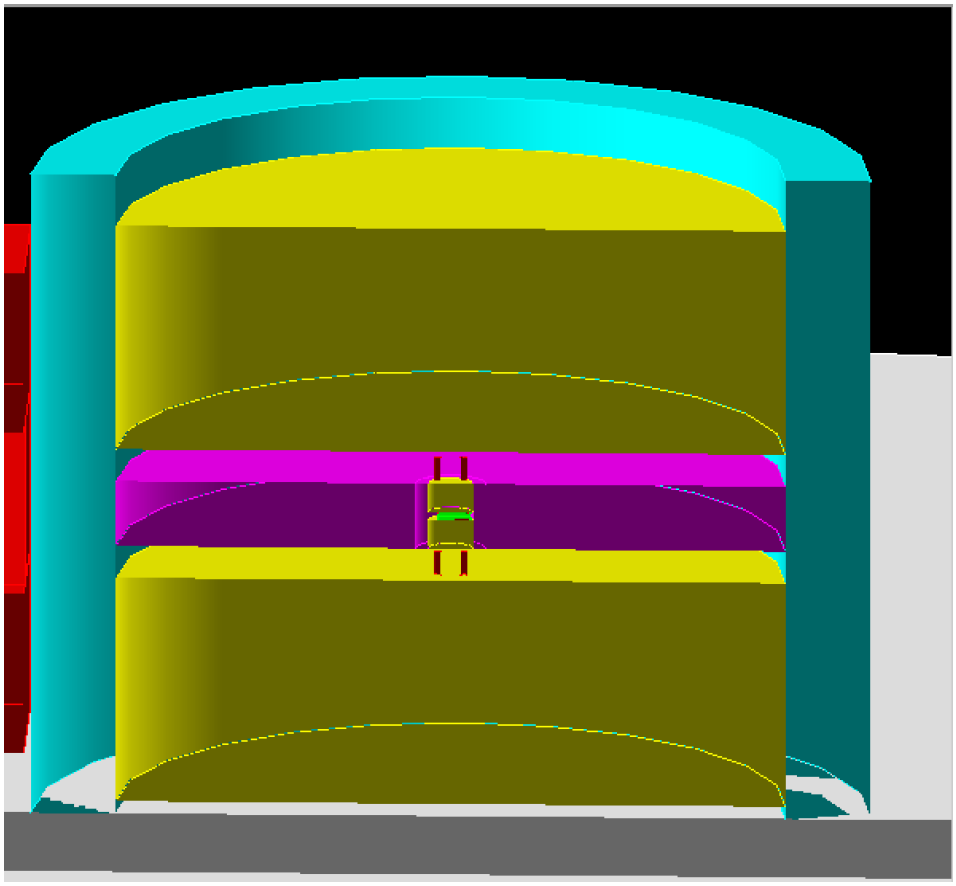

FIG. 1: A vertical cut through the SNS target hall, zoomed into the target region. The green structure at the center of the figure represents the main SNS target, small yellow structures above and below the target are the upper and lower Be-plugs, magenta structures are the stainless steel reflectors, 4 red ticks represent the moderators, large yellow structures are the upper and lower steel plates, and the cyan cylindrical surrounding represents the concrete wall. The red structure on the left is proton beam line shielding.

III. SIMULATION DETAILS

In this section, we discuss major components of our simulation.

A. Target Hall and Target Geometry

The SNS target has a complicated geometry involving several different components many of which are inconsequential when discussing neutrino production. For the baseline simulation, we implemented a simplified version of this geometry. The world volume for our simulation was taken to be a 300-m-radius sphere filled with air. A 39.9 cm $\times$ 10.4 cm $\times$ 50 cm liquid Hg target is placed at (0, 0, -5 cm) so that upstream face of the target is at z=+20 cm and downstream face of the target lies at z=-30 cm with respect to the center of the world volume. The target is encased by six 0.52-cm-thick steel plates. The target box is sandwiched between two 45-cm-high Beryllium plugs of radius 35 cm. The upper and lower Be plugs rest at 28.3 cm from the target center. The geometry also includes inner and outer stainless steel shielding along with upper and lower steel plates. Two moderators, modeled as 36-cm-high cylinders of radius 5-cm filled with liquid hydrogen, are placed 74 cm below the target center at z = $\pm$ 20 cm. A similar cylinder filled with LH_2 is placed above the target at 74 cm at z = -20 cm. Another similar cylinder filled with liquid water is placed at z = 20 cm. The area near the target region is surrounded by a cylindrical concrete room. The steel shielding around the proton beamline is also included. Fig. 1 shows a vertically sliced view of the SNS target region.

We implemented following three detectors that are currently being considered by planned neutrino experiments to be carried out at SNS [2, 3] .

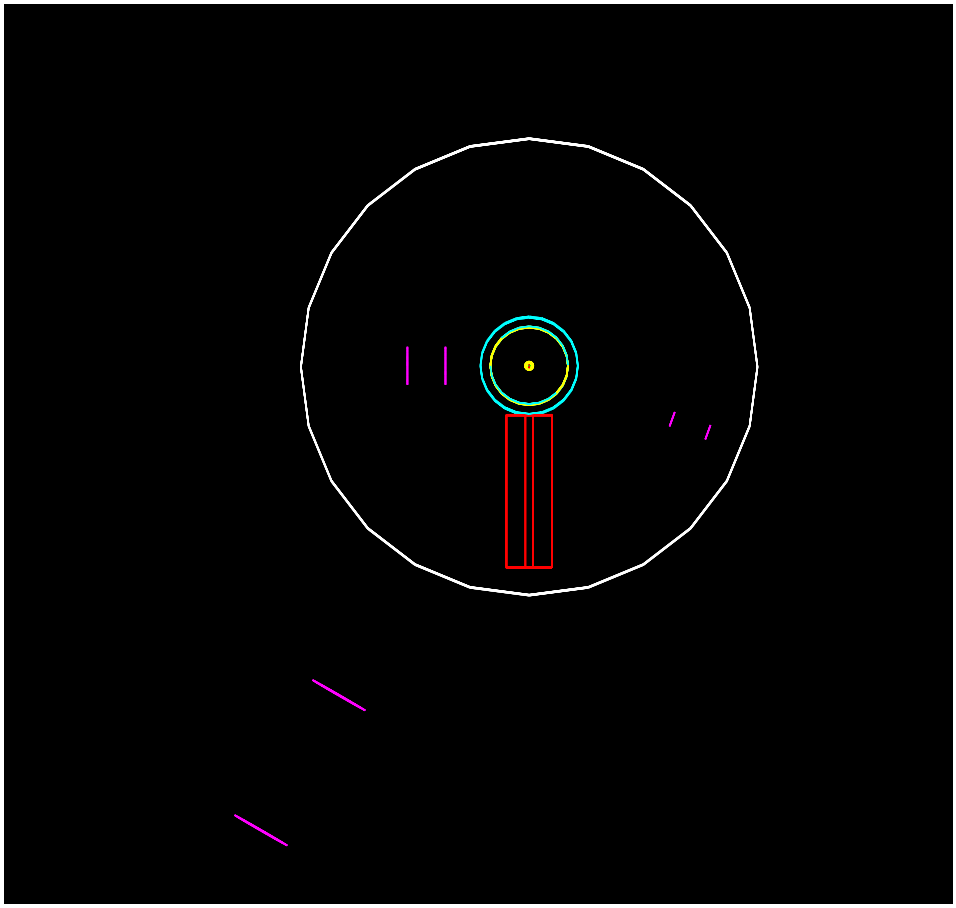

FIG. 2: Wire frame diagram showing overhead view of the SNS target hall. The magenta line frames represent different detectors, red lines represent upstream beamline shielding, cyan circles represent concrete room, and the while circles show the concrete floor of the target hall. The yellow dot represents the target region.

1. OscSNS Far Detector: A 20.5-m-long, 8-m-diameter cylinder, representing the proposed OscSNS detector, is placed 50 m away from the target center in the backward direction at 150° with respect to the initial beam direction.

2. Near Detector: A 5-m-long, 5-m-diameter cylinder, representing the proposed COHERENT detector, is placed 10 m away from the target center in the backward direction at 90° with respect to the initial beam direction.

3. Basement Detector: A 5-m-long, 1-m-diameter cylinder is placed in the ground floor at 20 m from the target center. The detector lies at an angle of -110° with respect to the initial beam direction.

A bird's eye view wireframe diagram of the SNS target hall along with the detector layout as implemented in our simulation is shown in Fig. 2. Currently these detectors are vacuum, and are included for the purpose of rate estimate only. For the moment, we do not simulate any physics interaction in these detectors.

B. Physics Lists

In GEANT4, secondary particle generation and their interactions are handled by physics lists containing predefined list of physics processes, models, and interactions the particles are allowed to be engaged in. Based on energy of the particle, appropriate electromagnetic and hadronic models are chosen to describe secondary particle produced in the interaction. The interactions at low energy (<150 MeV) are described by pre-compounded models, where as the interaction at high energy (> 10 GeV) are described by either by Fritiof model or the quark-gluon string model. Medium energy interactions are described by Bertini (BERT), Binary (BIC), or the Liege intra nuclear cascade models.

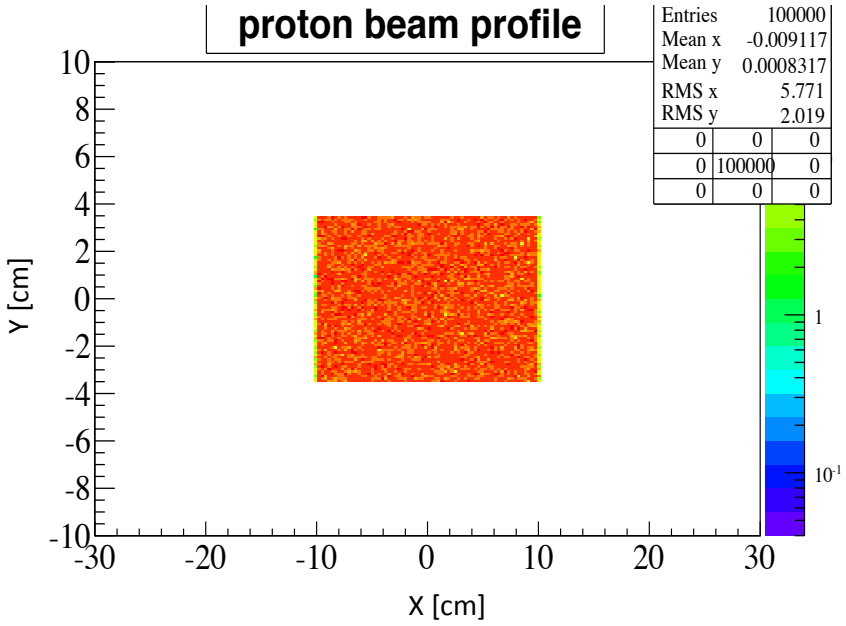

FIG. 3: Beam profile of the simulated 100 k protons on target

A complete physics list contains a combination of these models to describe particle interactions at all energies. Table I shows a comparison of physics lists in terms of the interaction models invoked at each approximate energy regime.

TABLE I: Model used by different physics lists

physics list	Low energy E < 150 MeV	Medium Energy 150 MeV < E <10 GeV	High energy E >10 GeV
QGSP_BERT	Precompounded	Bertini cascade	Quark-gluon string
FTFP_ BERT	Precompounded	Bertini cascade	Fritiof
QGSP_ BIC	Precompounded	Binary cascade	Quark-gluon string
QGSP_ INCLXX	Precompounded at very low energy	Liege intracnuclear (INCL++) + ABLA handles energy range 1 MeV-3 GeV	Quark-gluon string

QGSP_BERT physics list uses pre-compounded model at projectile energies below 150 MeV, the Bertini cascade model for primary protons, neutrons, pions and kaons at medium energy (below ∼10 GeV), and quark-gluon string model at energies above 10 GeV. Similarly, FTFP_BERT uses a combination of pre compounded, Bertini, and the Fritiof models to describe particle interaction at low, medium and high energies. The INCLXX variants of the QGSP_* and FTFP_* physics lists use and Abrasion/Ablation (ABLA) models to simulate particle interactions at low to medium energy (1 MeV to 3 GeV). We started with the QGSP_BERT since it was validated in earlier simulation efforts [2]. We ran our simulation with BERT, BIC, and the INCLXX variants of the QGSP_* physics lists. We also tested BERT and INCLXX variants of the FTFP_* physics list.

C. Primary Proton Beam

General Particle Source (GPS) in GEANT4 provides a framework to configure the primary proton beam. 1 GeV mono-energetic protons, distributed within a rectangle of 20 cm × 7 cm cross sectional area, were shot perpendicularly on to the front face of the target (z=+20 cm) along the negative z-direction. The proton beam has a gaussian distributions in x ($\sigma_x = 5$ cm) and y ($\sigma_y = 1.75$ cm). At the moment, the beam pulse timing structure is not included in our simulation. Fig. 3 shows the profile of the generated proton beam.

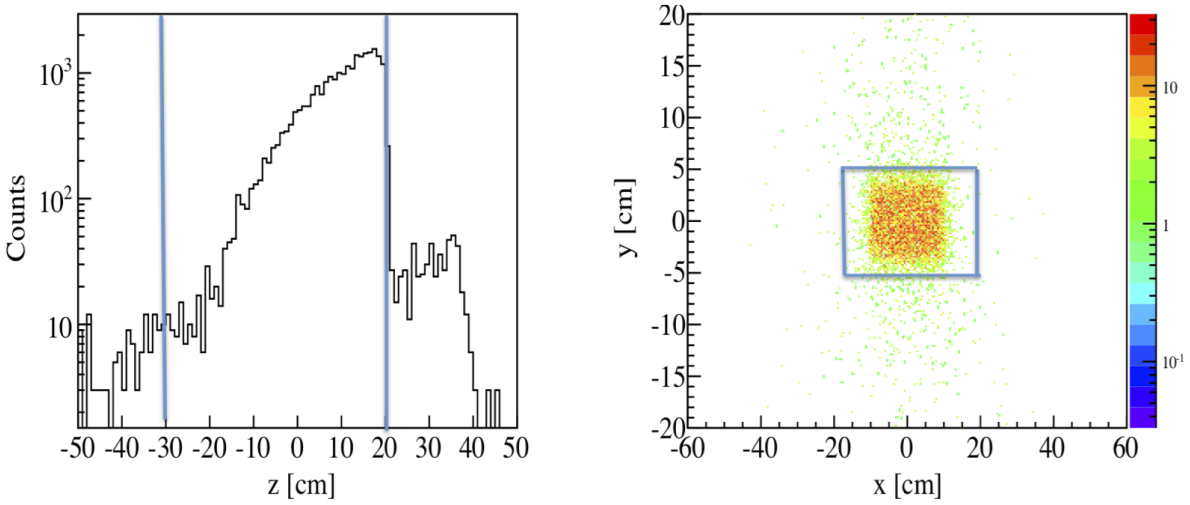

FIG. 4: Spatial distribution of point of origin of all types of neutrinos.

D. Counters and Histograms

The interaction of the proton beam with liquid Hg target creates secondary charged mesons, which successively decay into charged leptons and neutrinos in the scheme given by Eqs. 1 and 3. We have several counters to keep track of secondary particle production and death processes. We also keep track of physics processes that the particles are engaged during its life time. We made histograms of relevant physical quantities including primary and secondary particle energy, their creation time, and their life time. In the following section, we discuss some important physical quantities that were studied.

1. Neutrino Profile at Production

Fig. 4 shows profile of the neutrinos at their point of origin. The plot on the left shows the distribution of neutrino point of origin along z-axis. The vertical lines represent approximate target position (50 cm long). The plot on the right shows x-y distribution of the point of origin of the neutrinos. The rectangular box represents approximate x and y dimensions of the target. It is obvious that some neutrinos are produced outside of the target. Further investigation of the neutrinos produced outside of the target indicates that the particles escape target and decay at rest in some other material outside of the target.

2. Particle Emission Time

The particle emission time is referred as the time elapsed since primary proton mercury interaction until secondary particles are created. We obtained the emission time from GEANT4 global time of the particle track. Fig. 5 shows the emission time spectra of pions/muons. The emitted time spectra of the different flavors of neutrino is shown in Fig. 6. It is clear for these figures that most of the neutrinos are emitted within a few micro seconds relative to the proton-Hg interaction.

3. Particle Life Time

The life time of a particle track is the time period between its creation to destruction. A particle is stopped and killed if either its kinetic energy falls to zero or if it leaves the world volume. We obtained particle life time from the G4 local time of the particle track. We plotted the life time distribution for neutrinos as well as other secondary particles that were produced. Figs. 7 and 8 show life time of at rest decay of π^+ and μ^+ respectively. We fitted an

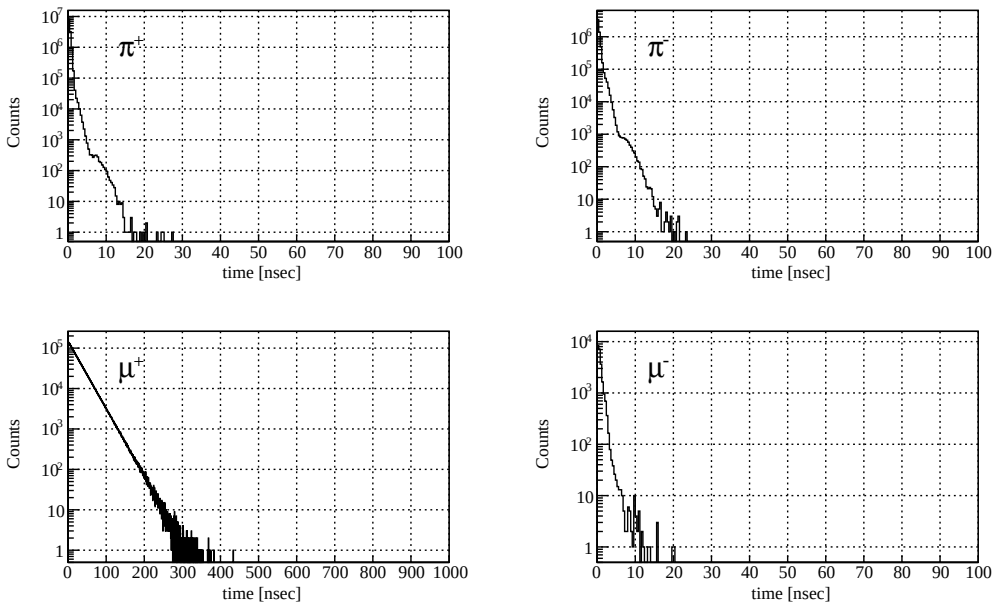

FIG. 5: The time since p+ Hg interaction to the emission of π^+ (top left), π^- (top right), μ^+ (bottom left), μ^- (bottom right).

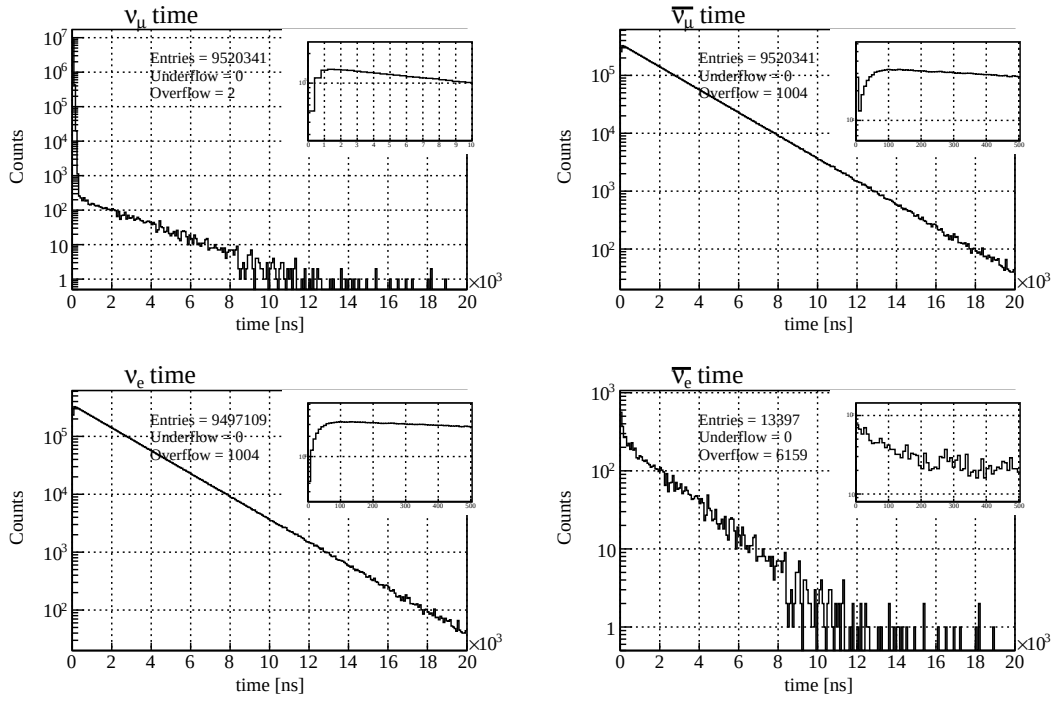

FIG. 6: The time spectra of emission of ν_μ (top left), $\bar{\nu_\mu}$ (top right), ν_e (bottom left), $\bar{\nu_e}$ (bottom right). The figures on the inset of each plot are the zoomed in view at the lower region of the original time spectra.

exponential function to these distributions to obtain average life time.The average life times of the π^+ and μ^+ from the exponential fit were found to be 26.1 $\pm$ 0.1 and 2202.9 $\pm$ 6.1 ns respectively. The nominal decay DAR life times of π^+ and μ^+ are 26 ns and 2200 ns respectively.

Assuming neutrino speed to be equal to the speed of light ($\sim$ 0.3 m/ns), a neutrino, produced at the center of a sphere of radius 300 m, will exit the surface of the sphere in 1000 ns. Hence, the neutrino life time distribution should

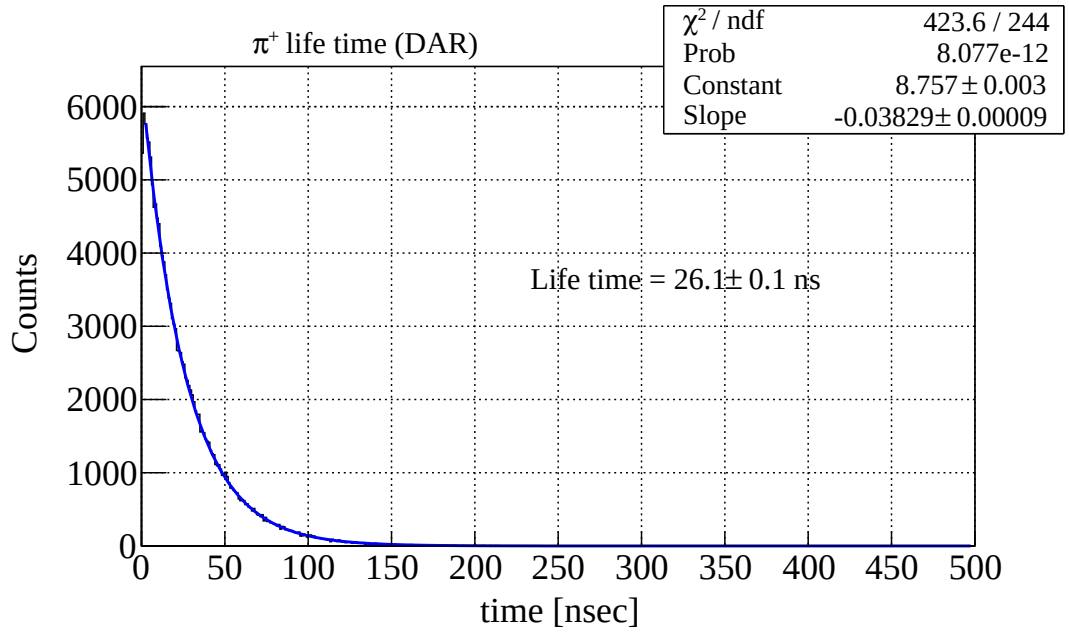

FIG. 7: π^+ lifetime distribution. The blue solid line represents the exponential fit to the distribution.

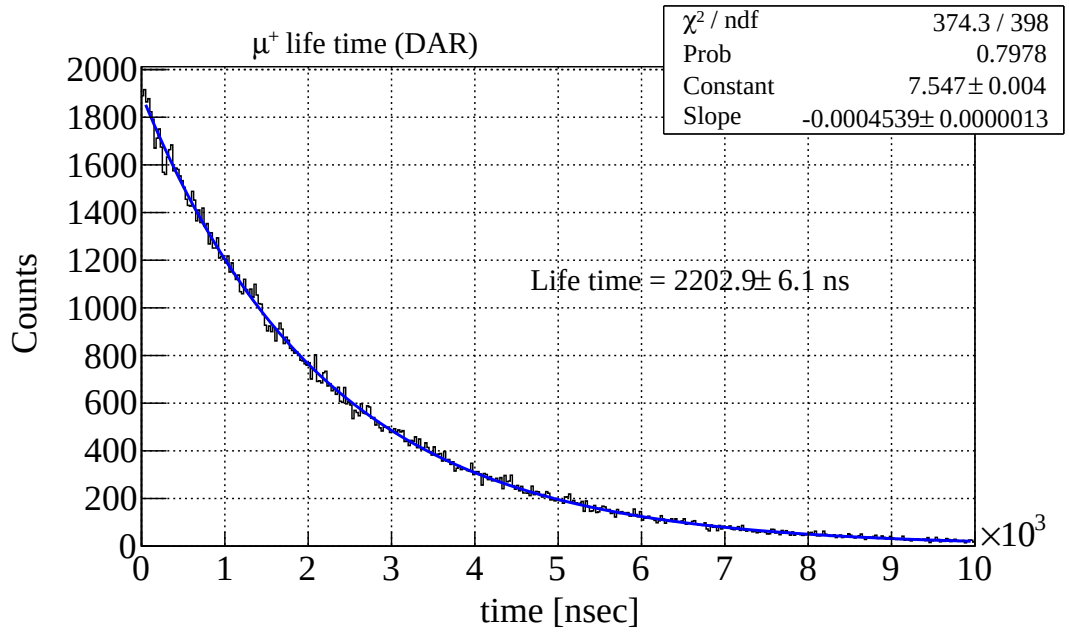

FIG. 8: μ^+ lifetime distribution. The blue solid line represents the exponential fit to the distribution.

be sharply peaked at 1000 ns. Fig. 9 shows the lifetime for each neutrino flavors. As expected, the life time for all neutrino species are roughly the same, and correspond to the expected flight time of the neutrinos inside the world volume. The width in the life time distribution for $\bar{\nu_e}$ is due to the $\bar{\nu_e}$'s produced by neutron decay outside of the target.

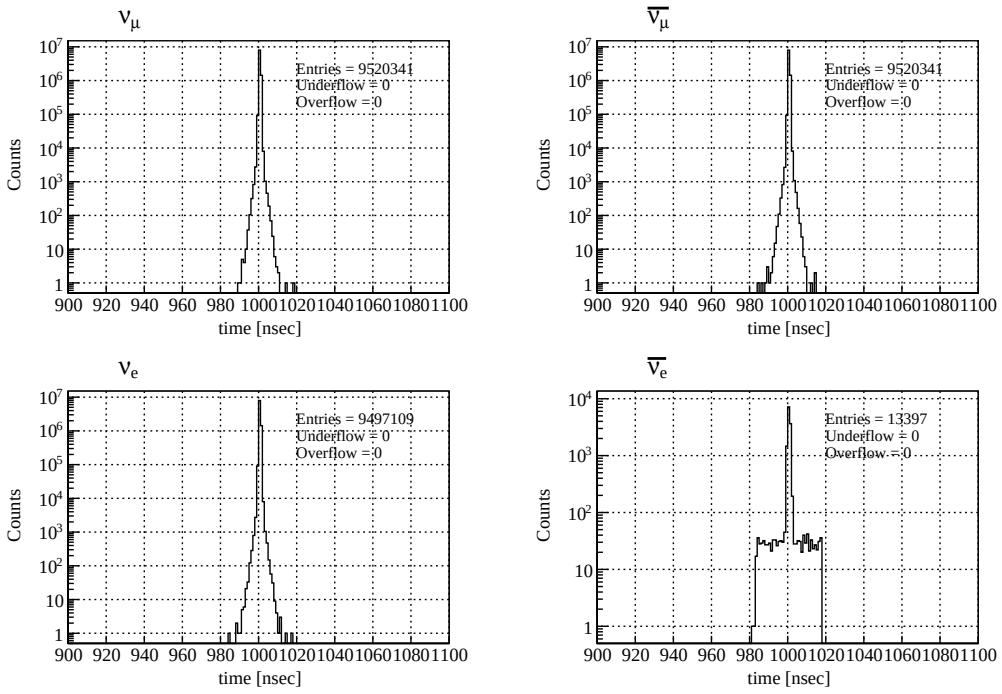

FIG. 9: The life time spectra of ν_μ (top left), $\bar{\nu_\mu}$ (top right), ν_e (bottom left), $\bar{\nu_e}$ (bottom right). As expected, most of the neutrinos live ≈1000 ns in the world volume.

4. Global Existence Time

Time elapsed since p+Hg interaction (t = 0) until the the particle is killed by decay process is referred as the global existence time of the particle. The time is obtained from the GEANT4 global time of the particle when it decays. Fig. 10 represents the global existence time for particles, which decay at rest or decay in flight. The mean global existence time is displayed in the top right corner of each plot.

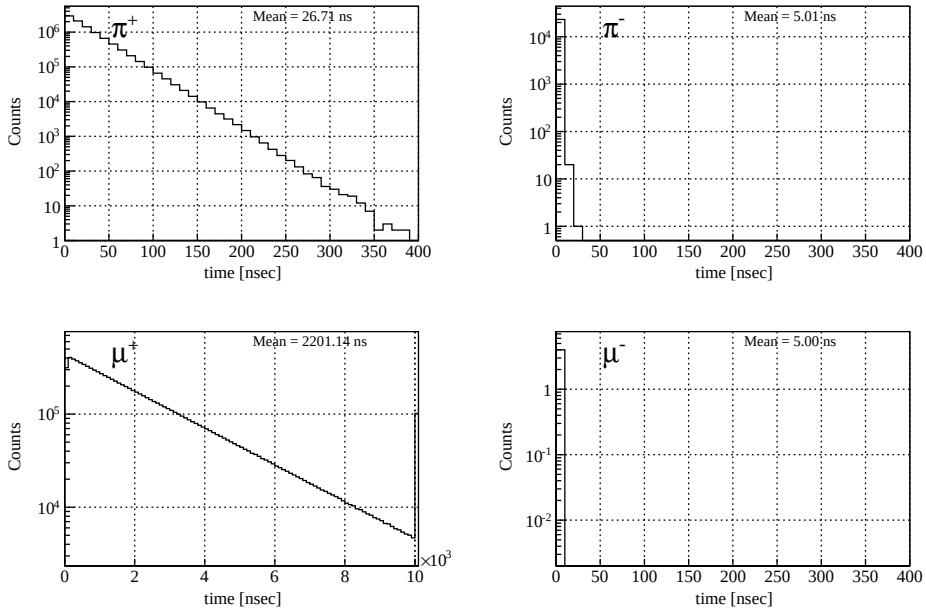

FIG. 10: The global existence time of π^+ (top left), π^- (top right), μ^+ (bottom left), μ^- (bottom right)

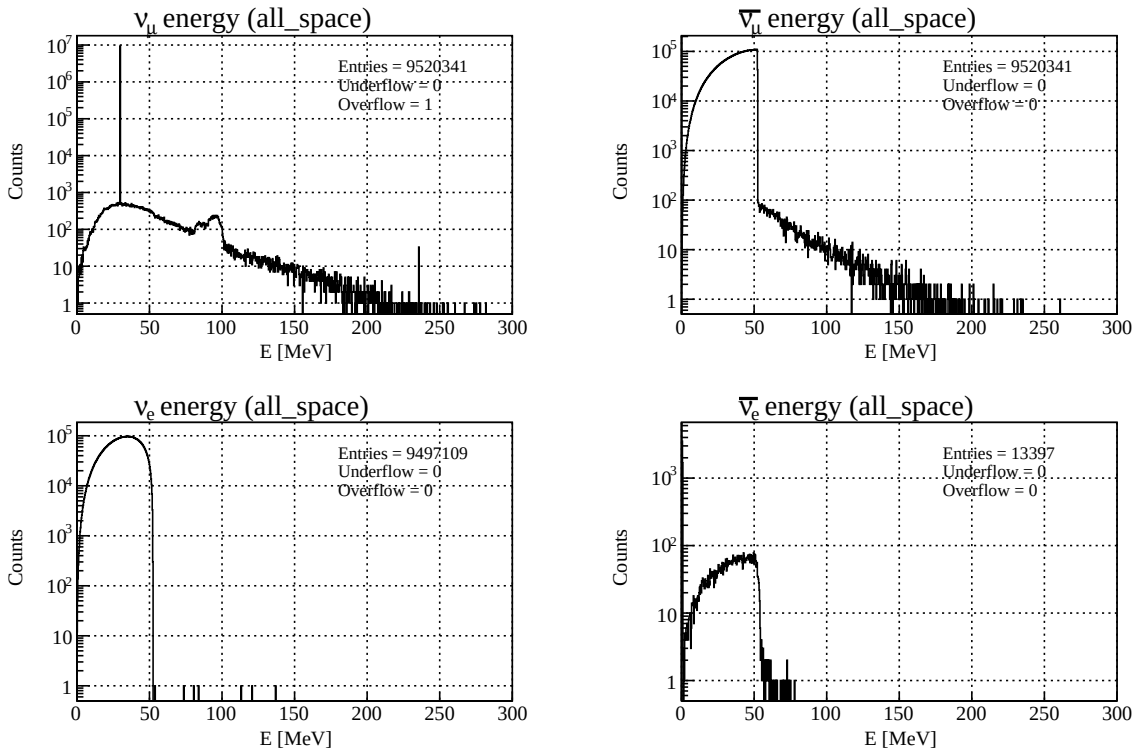

FIG. 11: The energy spectra all produced neutrinos ν_μ (top left), $\bar{\nu_\mu}$ (top right), ν_e (bottom left), $\bar{\nu_e}$ (bottom right) (include both DAR and DIF components). The peak at 30 MeV on ν_μ energy distribution is the neutrino energy corresponding to π^+ decay at rest, while another structure at approximately 95 MeV is the neutrino energy from μ^- capture at rest process.

5. Neutrino Energy Spectra

The energy of the neutrino produced via pion decay at rest depends only on the mass of the pion and the muon, and is given as:

$$E_\nu = \frac{m_\pi^2 - m_\mu^2}{2m_\pi}, \tag{5}$$

which yields $E_\nu \approx 29.8$MeV. Similarly using three body decay kinematics it can be shown that the energy of the neutrinos from muon decay at rest will be in the range of 0-52 MeV. The energy distribution of different flavors of neutrinos produced in our simulation are shown in Fig. 11. The prominent peak at ≈ 30 MeV on the ν_μ energy distribution corresponds to neutrino energy from π^+ decay at rest. The other structure at around 95 MeV corresponds to the neutrinos energy from a model dependent process known as μ^- capture at rest process. A small fraction of neutrinos, which are produced from pion/muon decay in flight, also contribute to the total energy flux. The energies of these neutrinos depend upon the energy (at decay) of the decaying particles. It is to be noted that both DAR and DIF components of pion/muon are included in the energy distributions shown in Fig. 11.

6. Kinetic Energy of DIF particle

Fig. 12 shows the kinetic energy of the particle when it decays in flight. As most of the pions/muons decay at rest, there are very few pions/muons left to decay in flight.

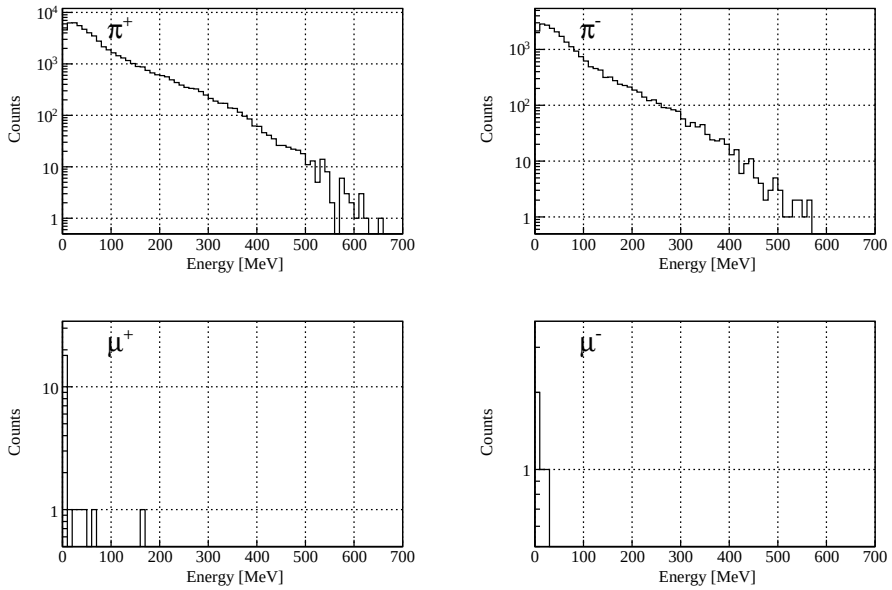

FIG. 12: Kinematic energy at the instant the particle decays in flight.

IV. RESULTS

A. Neutrino Flux

Neutrino energy flux distribution in the near, OscSNS, and the basement detectors are shown in Fig. 13, 14, and 15 respectively. It is clear from the figures that almost all of the neutrinos reaching these detectors are the product of pions/muons DAR.

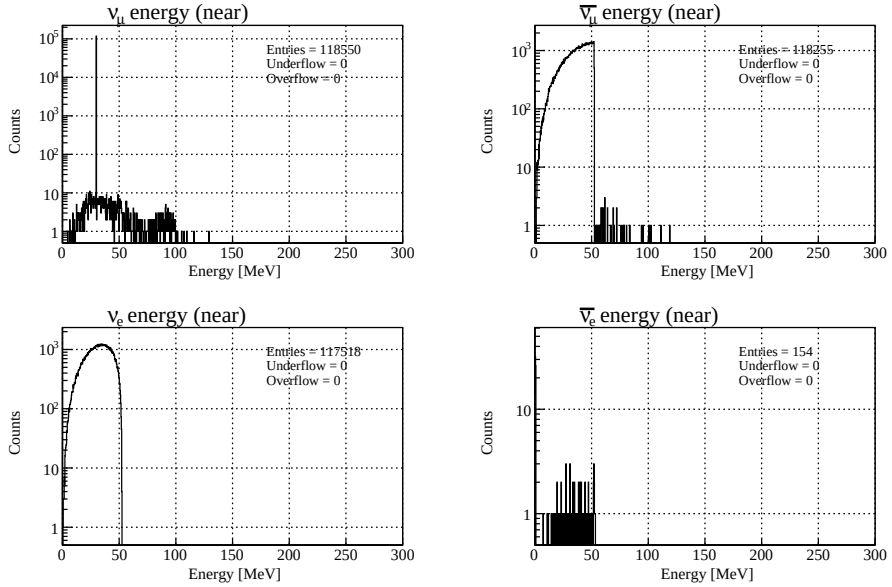

FIG. 13: Energy spectra of neutrinos ν_μ (top-left), $\bar{\nu_\mu}$ (top-right), ν_e (bottom-left), $\bar{\nu_e}$ (bottom-right) detected in the near detector

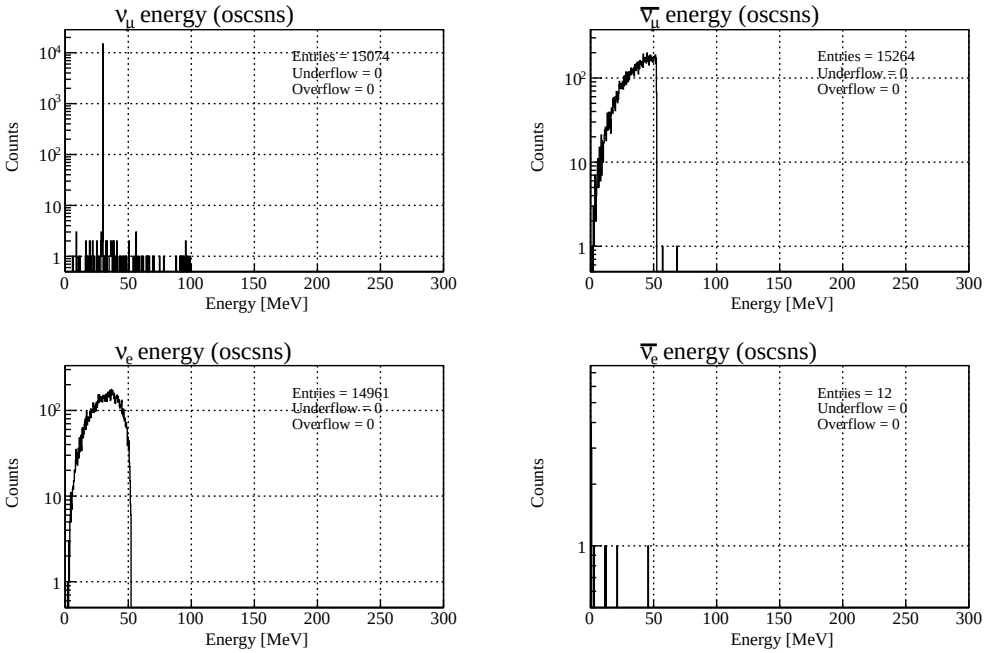

FIG. 14: Energy spectra of neutrinos ν_μ (top-left), $\bar{\nu_\mu}$ (top-right), ν_e (bottom-left), $\bar{\nu_e}$ (bottom-right) detected in the OscSNS detector

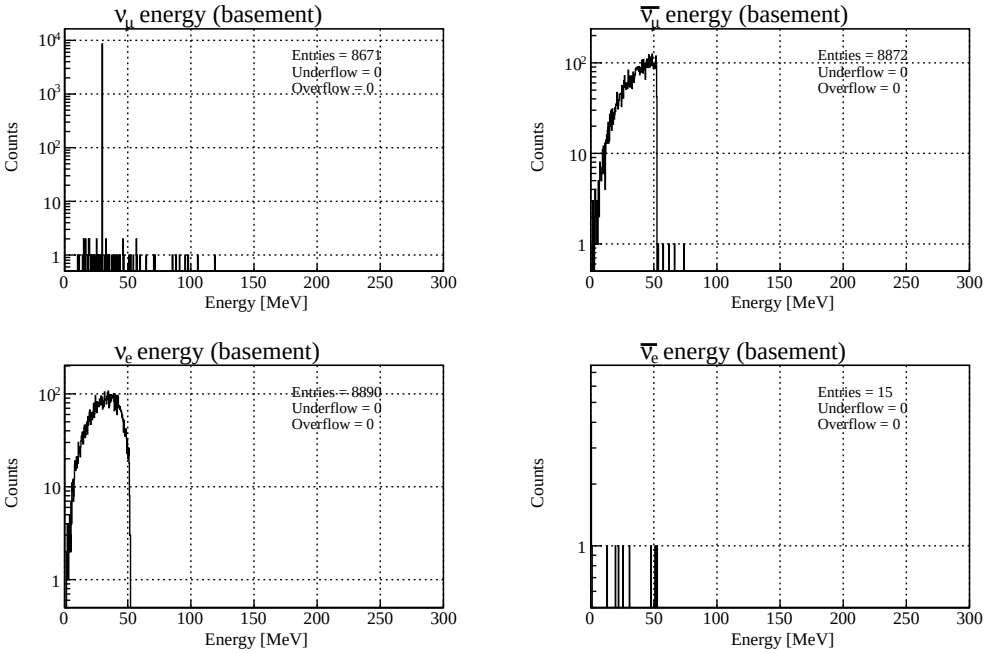

FIG. 15: Energy spectra of neutrinos ν_μ (top-left), $\bar{\nu_\mu}$ (top-right), ν_e (bottom-left), $\bar{\nu_e}$ (bottom-right) detected in the basement detector

Similarly Fig. 16, 17, and 18 show the time elapsed between creation and detection of the neutrinos at near, OscSNS, and the basement detector respectively. These distribution also include neutrinos from both DAR and DIF components of π/μ decay.

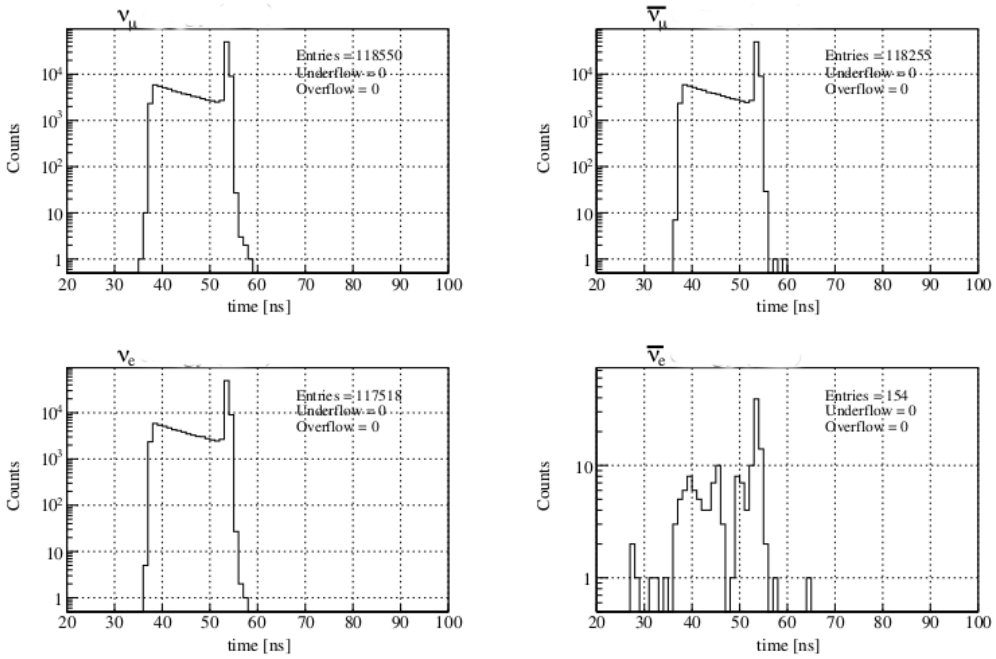

FIG. 16: Time spectra of different flavors of neutrinos detected in the near detector

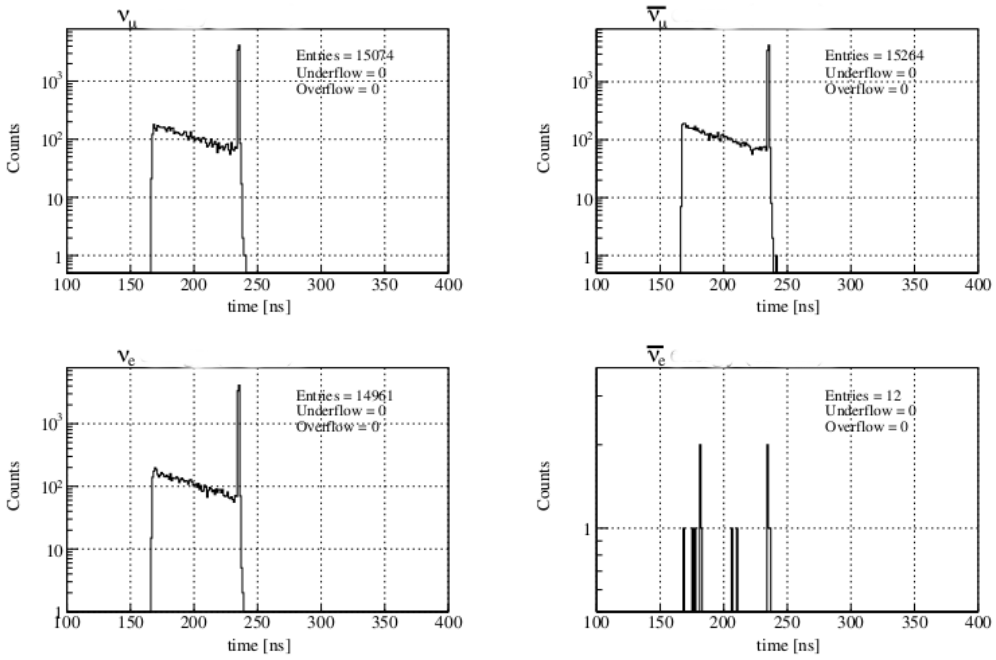

FIG. 17: Time spectra of different flavors of neutrinos detected in the OscSNS detector

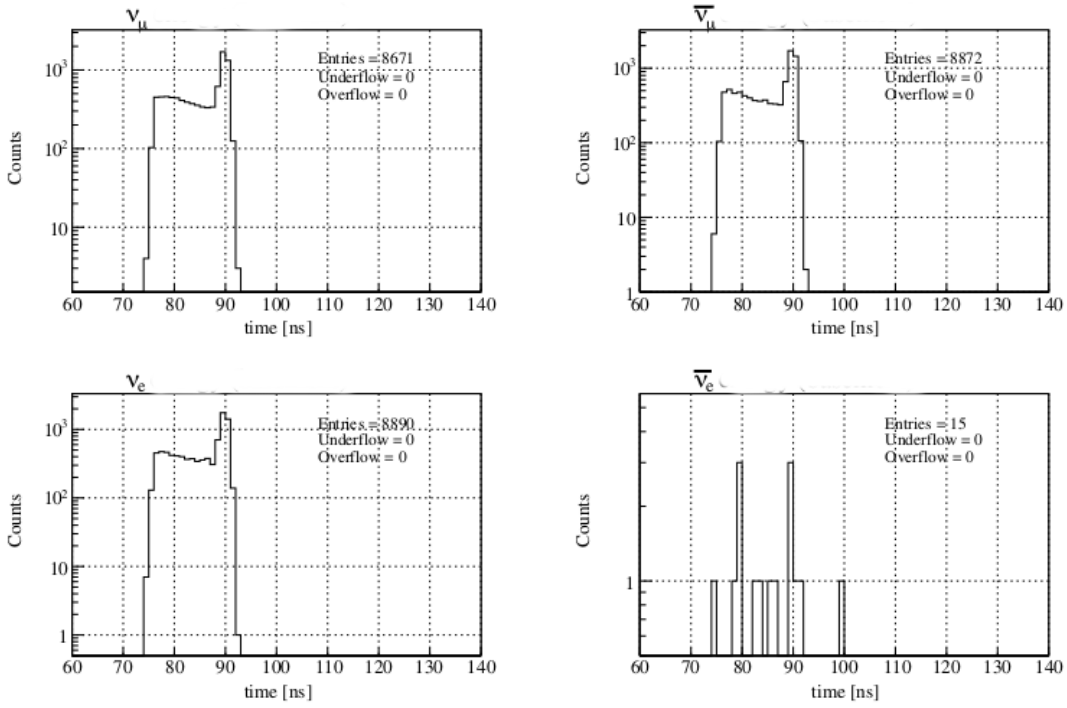

FIG. 18: Time spectra of different flavors of neutrinos detected in the basement detector

B. Physics List Comparison

The results presented until now were obtained using QGSP_BERT physics list. To study model dependency, we ran our simulation for FTFP_BERT physics list which uses Fritiof model instead of the quark gluon string model at high energy but uses same Bertini cascade model at the medium energy. Ideally, the results for FTFP_BERT and QGSP_BERT are expected to be same in our energy regime ($\approx$ 1 GeV) since both physics lists invoke same nuclear cascade model. We also ran our simulation for QGSP_BIC physics list, which uses same quark gluon string model at high energy but uses binary cascade model at the medium energy. For each physics list, we simulated 1.14×10^8 protons on target.

Table II summarizes total number of neutrinos produced and also the number of neutrinos recorded in each detector for different physics lists. As expected, QGSP_BERT and FTFP_BERT results are very similar. The minimal difference is caused by the difference in random number sequence as different random number seeds were used. However, the results for QGSP_BIC sharply differs from the other two. The difference is likely the result of underlying physics differences between two models, which are discussed further in the next section.

C. Upgrade to GEANT4 10.1

A newer version of GEANT4 (4.10.1) was released at the beginning of December, 2014, which had major improvements in the implementation of Bertini and binary cascading models in G4 hadronic processes. The newer version had significant improvements in the implementation of Fritiof and the quark gluon string models. Moreover, earlier versions of GEANT4 didn't have a good way to know the muon stopping subprocesses responsible for creating secondary particle tracks from μ^- tracks. The creator process for all such tracks were assigned to be muMinusCaptureAtRest even though the tracks were creating by bound decay of μ^-. The newer version of GEANT4 provided the functionality to access information about the subprocesses creating these tracks. The newer version also included newer version of INCL++ (v5.28). We upgraded to GEANT4.10.1 to utilize these latest features.

We re-ran our simulation for different variants of QGSP physics lists, namely, QGSP_BERT, QGSP_BIC and QGSP_INCLXX to compare models applicable to SNS energy regime. GEANT4 physics reference manual states that the Bertini cascade model treats target nucleus as an nuclear medium and solves Boltzman equation on average. The excitons (particle-hole states) are added to the nuclear medium after each collision [4]. In contrast, the Binary cascade

TABLE II: Comparison between different physics lists

physics list	POT	Neutrino Type	Total	ν/POT	Near Detector	OscSNS Detector	Basement Detector
QGSP BERT	1.14×10^8	ν_μ	9520341	0.084	118550	15074	8671
		$\bar{\nu_\mu}$	9520341	0.084	118255	15264	8872
		ν_e	9497109	0.084	117518	14961	8890
		$\bar{\nu_e}$	13397	0.0001	154	12	15
FTFP BERT	1.14×10^8	ν_μ	9533307	0.084	118319	15556	8637
		$\bar{\nu_\mu}$	9533307	0.084	118711	15401	9017
		ν_e	9509954	0.084	119449	15111	8826
		$\bar{\nu_e}$	13374	0.0001	163	20	19
QGSP BIC	1.14×10^8	ν_μ	18836692	0.17	235642	29638	17295
		$\bar{\nu_\mu}$	18836692	0.17	233666	30300	17229
		ν_e	18756296	0.17	231855	30290	17217
		$\bar{\nu_e}$	23685	0.0002	261	29	9

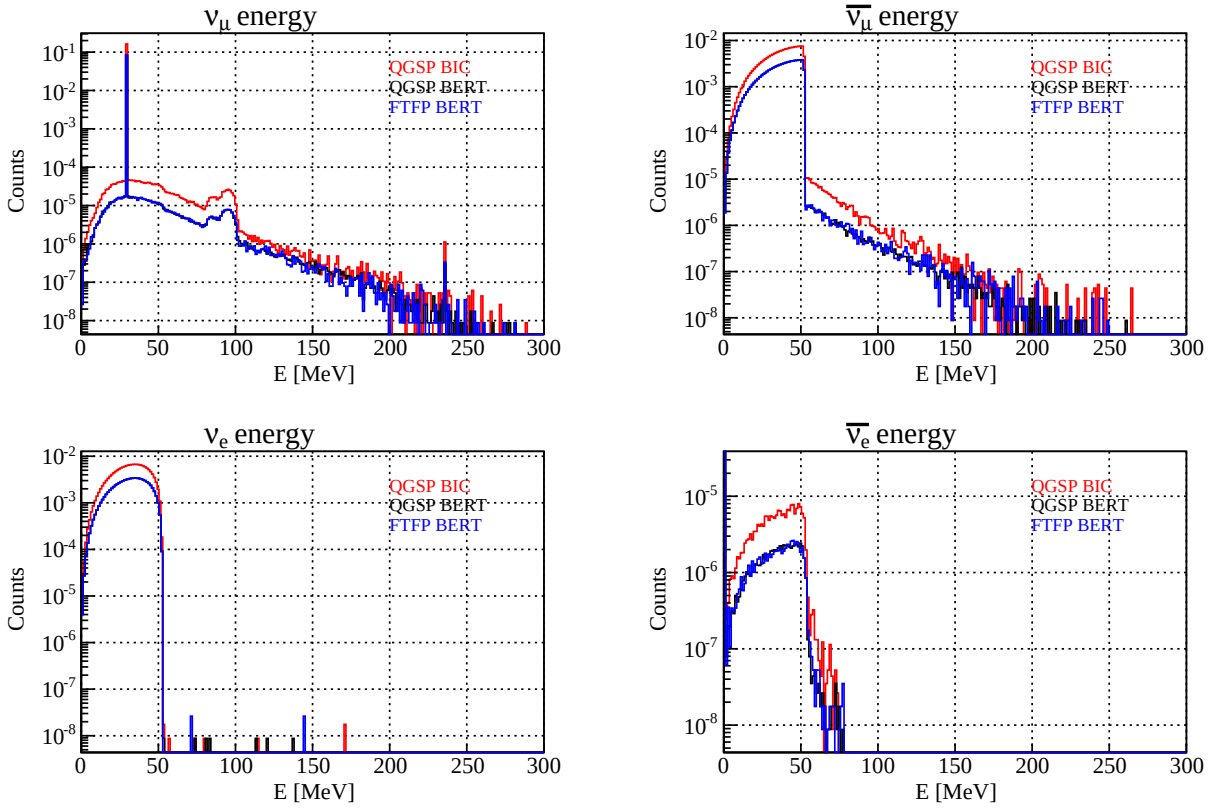

FIG. 19: Comparison of energy spectra of ν_μ (top-left), $\bar{\nu_\mu}$ (top-right), ν_e (bottom-left), $\bar{\nu_e}$ (bottom-right) for QGSP_BERT (black), QGSP_BIC (red), and FTFP_BERT (blue). All plots have 1.14 $\times 10^8$ of protons on target

model treats the target nucleus as a three dimensional collection of the nucleons. The hadron nucleon collisions are handled by forming resonances, which then decay according to their quantum numbers. The elastic scattering of the nucleons are also allowed [4]. The INCL++ is a C++ version of Liege cascade model and uses ABLA code for nuclear de-excitation. INCL++ is a promising model and is well validated against nuclear spallation data. However, its GEANT4 implementation and validation are still ongoing. Some important features of these physics lists are listed in Table III.

Fig. 20 shows the spectra of total produced neutrinos of each flavor. As discussed earlier, it is clear that the results for BERT and INCLXX are identical. However, the BIC spectra are not consistent with the other two spectra.

TABLE III: Comparison between different models that are relevant at the SNS energy regime

BERT	INCLXX	BIC
Applicable to proton, neutrons, pions, kaons, and hyperon in the energy range up to 10 GeV. Target nucleus is treated as an average nuclear medium. The excitons (particle-hole) states are added after each collision. Path lengths of the nucleons in the nucleus are sampled according to the local density and free nucleon-nucleon cross sections. In the end of the cascade, the excited nucleus is represented as a sum of particle hole states, which is then decayed by pre-equilibrium, fission, and evaporation method.	Applicable to nucleon-, pion- and light-ion-induced reactions in the kinetic-energy range up to 3 GeV. Generates final states for inelastic scattering of nucleons, pions and light nuclei on nuclei. Well tested for spallation studies. C++ version of Liege Intra-nuclear cascade. Uses ABLA code for nuclear de-excitation. Not applicable to light nuclei GEANT4 implementation is not yet well tested.	Applicable to p, n in energy range upto 10 GeV and for pions up to 1.3 GeV. Target nucleus is modeled as a three dimensional and isotropic object. The nucleons are placed in space according to nuclear density and the nucleon momentum is calculated according to Fermi gas model. The primary particles interact with nucleons in binary collisions producing resonances which decay according to their lifetime producing secondary particles. The secondary particles re-scatter with nucleons creating a cascade.

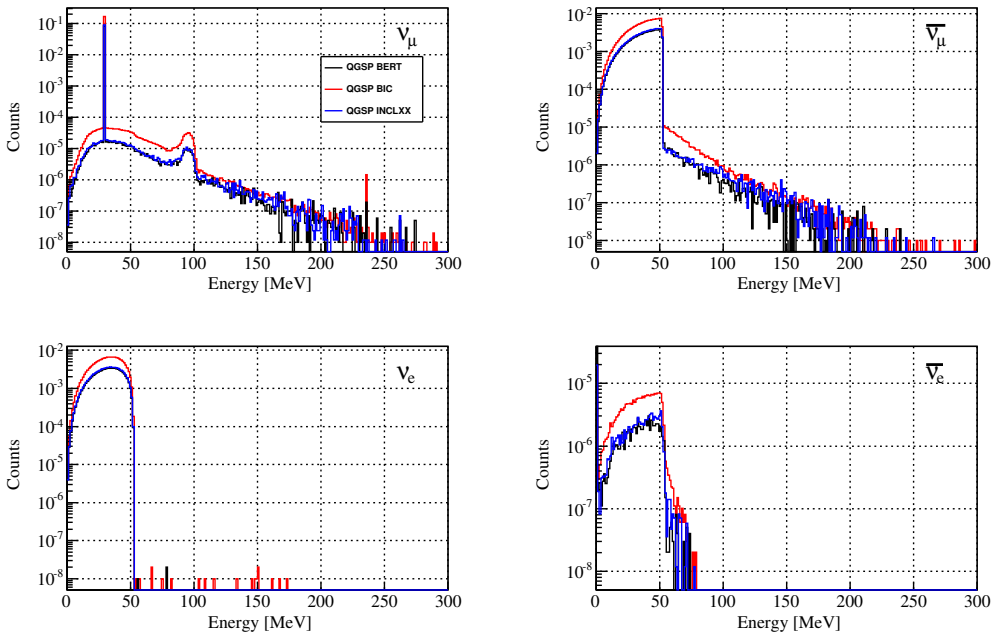

FIG. 20: Neutrino energy spectra of ν_μ (top-left), $\bar{\nu_\mu}$ (top-right), ν_e (bottom-left), $\bar{\nu_e}$ (bottom-right) for QGSP_BERT (black), QGSP_BIC (red), and QGSP_INCLXX (blue) physics lists. The curves are normalized to number of protons on target.

Table IV lists number of particles per proton on target for these physics lists. As discussed earlier, the Binary model has nearly double particles per proton than for other physics list. The realistic situation is believed to be somewhere between Bertini and INCLXX model [5].

TABLE IV: Comparison between different physics lists

particles/POT	QGCP_BERT	QGSP_BIC	QGSP_INCLXX
ν_μ	0.08389	0.16524	0.08953
$\bar{\nu_\mu}$	0.08389	0.16524	0.08953
ν_e	0.08368	0.16453	0.08930
$\bar{\nu_e}$	0.00011	0.00021	0.00010
secondary π^+	0.098	0.2030	0.1026
secondary π^-	0.037	0.1300	0.0482
secondary n	13.67	10.047	10.81
secondary p	2.7	1.94	2.08
π^+ DAR	0.08318	0.16321	0.008875
π^+ DIF	0.00050	0.00132	0.00055
π^- DAR	0	0	0
π^- DIF	0.00021	0.00071	0.00023
μ^+ DAR	0.08368	0.16453	0.08930
μ^+ DIF	0	0	0
μ^- DAR	0	0	0
μ^- DIF	0	0	0
μ^- Capture	0.00013	0.00039	0.00016
μ^- decay	0.00015	0.00052	0.00016

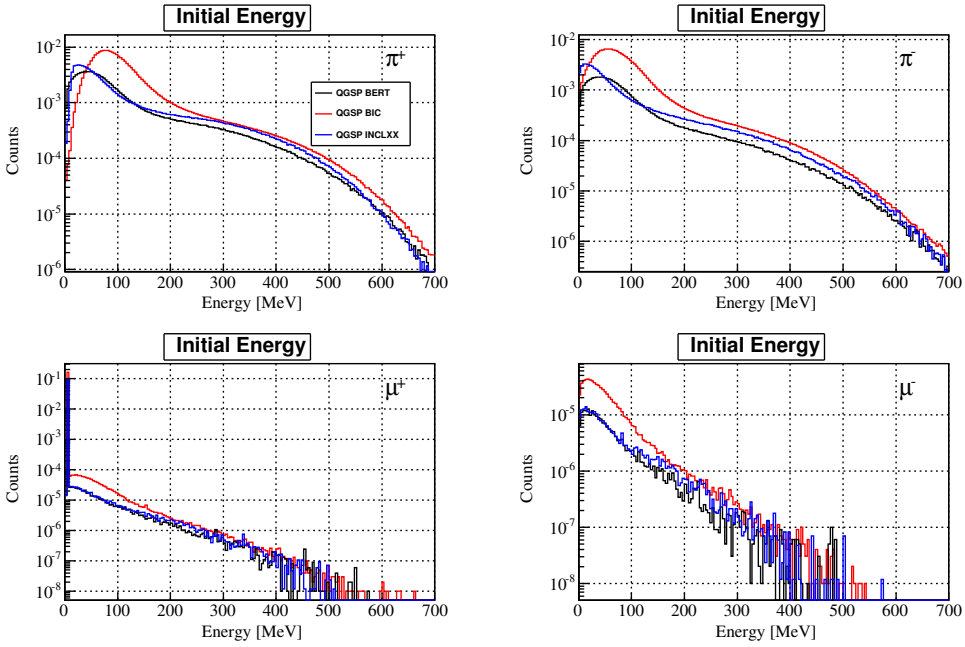

FIG. 21: Initial energy of π^+ (top-left), π^- (top-right), μ^+ (bottom-left), μ^- (bottom-right) that decay in flight. The curves represent physics lists: QGSP_BERT (black), QGSP_BIC (red), and QGSP_INCLXX (blue). The curves are normalized to number of protons on target.

Figs. 22 and 23 compare production time of different particles relative to p+Hg interaction (t = 0) for different physics lists. These plots also indicate that the binary results are considerably different than other two.

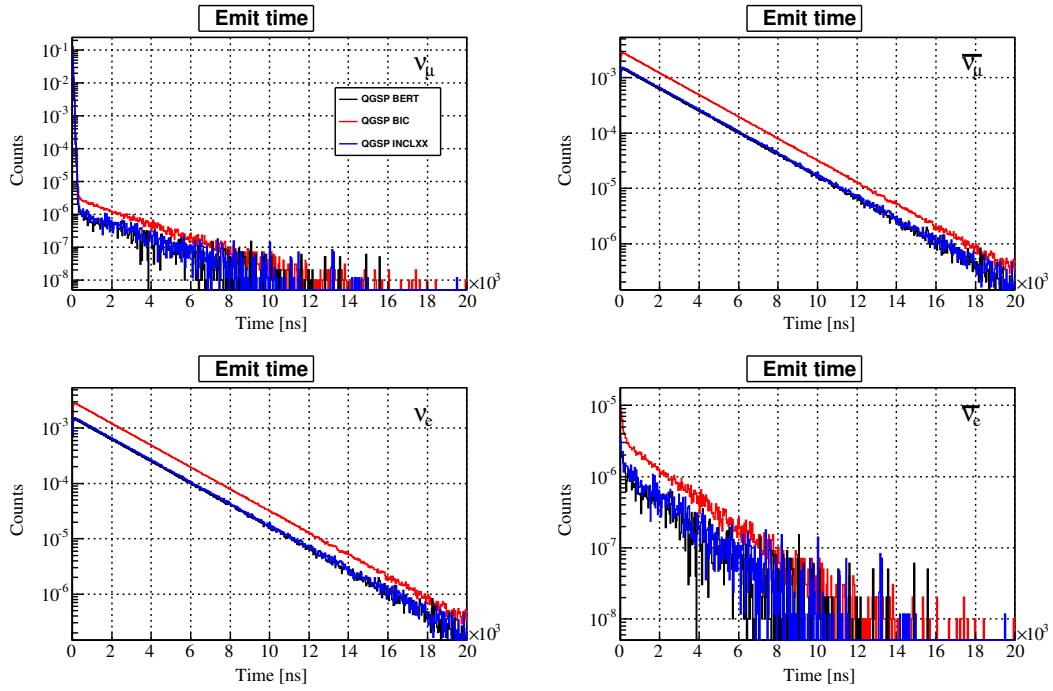

FIG. 22: Production time (relative to p+Hg interaction) of ν_μ (top-left), $\bar{\nu_\mu}$ (top-right), ν_e (bottom-left), $\bar{\nu_e}$ (bottom-right) for QGSP_BERT (black), QGSP_BIC (red), and QGSP_INCLXX (blue) physics lists. The curves are normalized to number of protons on target.

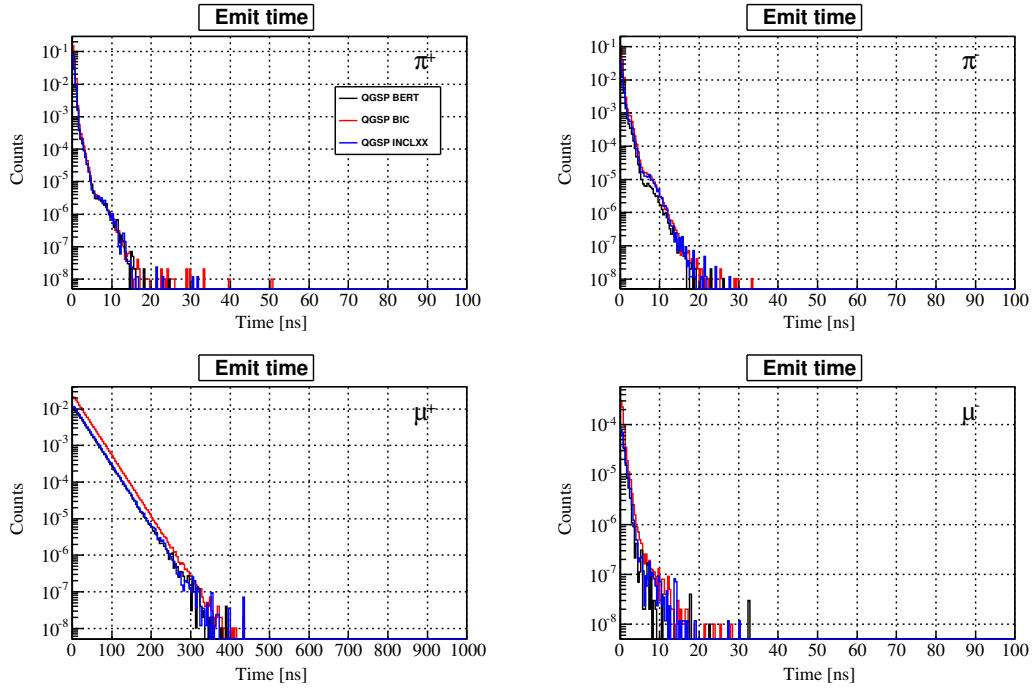

FIG. 23: Production time (relative to p+Hg interaction) of π^+ (top-left), π^- (top-right), μ^+ (bottom-left), μ^- for QGSP_BERT (black), QGSP_BIC (red), and QGSP_INCLXX (blue) physics lists. The curves are normalized to number of protons on target.

Figs. 24 and 25 show a comparison of life time of different particles for different physics lists. Similar difference in the physics list can be seen.

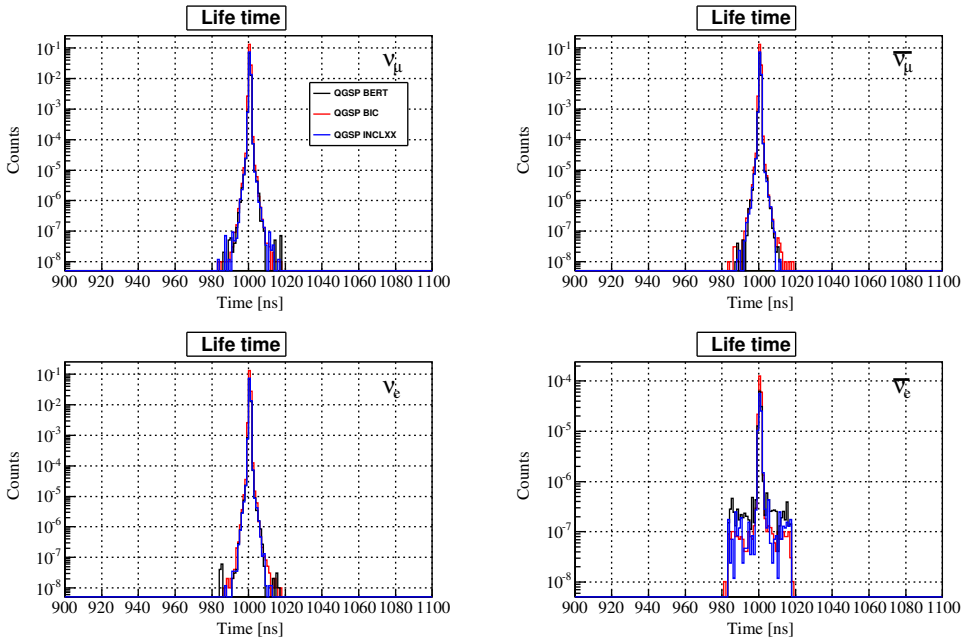

FIG. 24: Life time of ν_μ (top-left), $\bar{\nu_\mu}$ (top-right), ν_e (bottom-left), $\bar{\nu_e}$ (bottom-right) for QGSP_BERT (black), QGSP_BIC (red), and QGSP_INCLXX (blue) physics lists. The curves are normalized to number of protons on target.

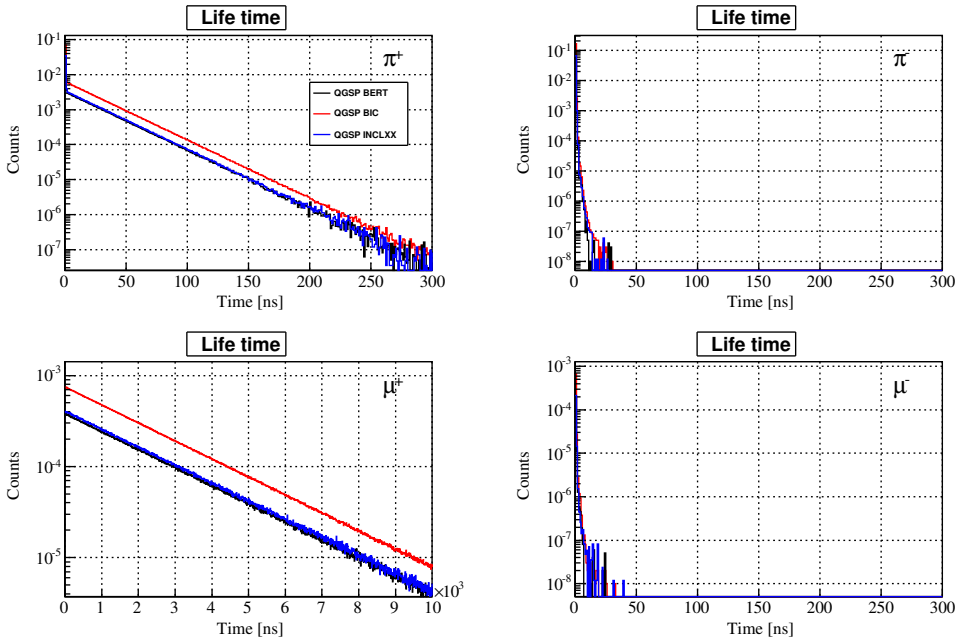

FIG. 25: Life time of π^+ (top-left), π^- (top-right), μ^+ (bottom-left), μ^- for QGSP_BERT (black), QGSP_BIC (red), and QGSP_INCLXX (blue) physics lists. The curves are normalized to number of protons on target.

V. SUMMARY

We have developed a baseline GEANT4 simulation package which will be useful for COHERENT, OscSNS, and other planned neutrino experiments at SNS. Using the simulation package, we estimated neutrino flux at various locations of interest near the SNS target area. We also compared different physics lists valid in the energy regime relevant to SNS operating energy. More results from this work can be found at `http://nflux.phys.ufl.edu/redmine/projects/2013-09-nuflux/wiki/Dipak`

Acknowledgements

This work was completed in part with resources provided by the University of Chicago Research Computing Center.

[1] *Spallation Neutron Source at ORNL*, `http://www.neutrons.ornl.gov/facilities/SNS/` (2014).
[2] M. Elnimr et al. (OscSNS Collaboration), arxiv **1307.7097** (2013).
[3] D. Akimov et al. (COHERENT Collaboration), arxiv **1310.0125** (2013).
[4] S. Agostinelli et al., Nuclear Instruments and Methods in Physics Research A **506**, 250 (2003).
[5] J. Yarba, private communication.